nature biomedical engineering

Article

https://doi.org/10.1038/s41551-025-01427-3

Scalable production of human cortical organoids using a biocompatible polymer

Received: 24 July 2023

Accepted: 12 May 2025

Published online: 27 June 2025

Check for updates

Genta Narazaki[1,2,6], Yuki Miura[1,2,6], Sergey D. Pavlov[1,2], Mayuri Vijay Thete[1,2], Julien G. Roth[2,3], Merve Avar[1,2], Sungchul Shin[2,4,5], Ji-il Kim[1,2], Zuzana Hudacova[1,2], Sarah C. Heilshorn[2,4] & Sergiu P. Pașca[1,2]

The generation of neural organoids from human pluripotent stem cells holds great promise in modelling disease and screening drugs, but current approaches are difficult to scale due to undesired organoid fusion. Here we develop a scalable cerebral cortical organoid platform by screening biocompatible polymers that prevent the fusion of organoids cultured in suspension. We identify a cost-effective polysaccharide that increases the viscosity of the culture medium, significantly enhancing the yield of cortical organoids while preserving key features such as regional patterning, neuronal morphology and functional activity. We further demonstrate that this platform enables straightforward screening of 298 FDA-approved drugs and teratogens for growth defects using over 2,400 cortical organoids, uncovering agents that disrupt organoid growth and development. We anticipate this approach to provide a robust and scalable system for modelling human cortical development, and facilitate efficient compound screening for neuropsychiatric disorders-associated phenotypes.

Human pluripotent stem cell-derived three-dimensional (3D) neural culture methods can be used to study human brain development and to investigate neuropsychiatric disease[1–3]. Current approaches to derive neural organoids involve either embedding of individual organoids into extracellular matrices or culturing organoids in suspension[4,5]. We have previously developed an approach to model human cerebral cortical development using human induced pluripotent stem (hiPS) cell-derived regionalized neural organoids, called human cortical spheroids or human cortical organoids (hCO)[6,7]. We have shown that hCO, which are derived exclusively in suspension cultures without the use of extracellular matrices, recapitulate features of corticogenesis[8], can be reliably derived across multiple experiments and lines[9], and can be used to model environmental and genetic brain disorders[10–14]. Although this suspended culture approach is relatively straightforward to implement, maintaining neural organoids is time intensive and requires efforts to manually separate and avoid undesired fusion of organoids over time. This spontaneous fusion can often limit the derivation of organoids of uniform size and the scale of experiments.

To address this issue, we screened biocompatible polymers that can be added to culture medium to prevent fusion and enable culture of multiple organoids in a single well (Fig. 1a). We selected 23 candidate polymers on the basis of molecular weight, chemical structure, electrostatic charge and biocompatibility (see details in Supplementary Table 1).

Results

To develop our culture system, we supplemented the neural differentiation medium with each of our polymers starting at day 6. We evaluated the effect of each polymer by culturing 5 hCO in each well of a 24-well plate for 25 days and then counting the number of remaining hCO in each well (Fig. 1a). We found that culture medium supplemented with xanthan gum (XG), a biocompatible exo-polysaccharide widely used in

[1]Department of Psychiatry and Behavioral Sciences, Stanford University, Stanford, CA, USA. [2]Stanford Brain Organogenesis, Wu Tsai Neuroscience Institute, Stanford, CA, USA. [3]Institute for Stem Cell Biology and Regenerative Medicine, Stanford University, Stanford, CA, USA. [4]Department of Materials Science and Engineering, Stanford University, Stanford, CA, USA. [5]Department of Agriculture, Forestry, and Bioresources, Seoul National University, Seoul, Republic of Korea. [6]These authors contributed equally: Genta Narazaki, Yuki Miura. e-mail: spasca@stanford.edu

https://doi.org/10.1038/s41551-025-01427-3

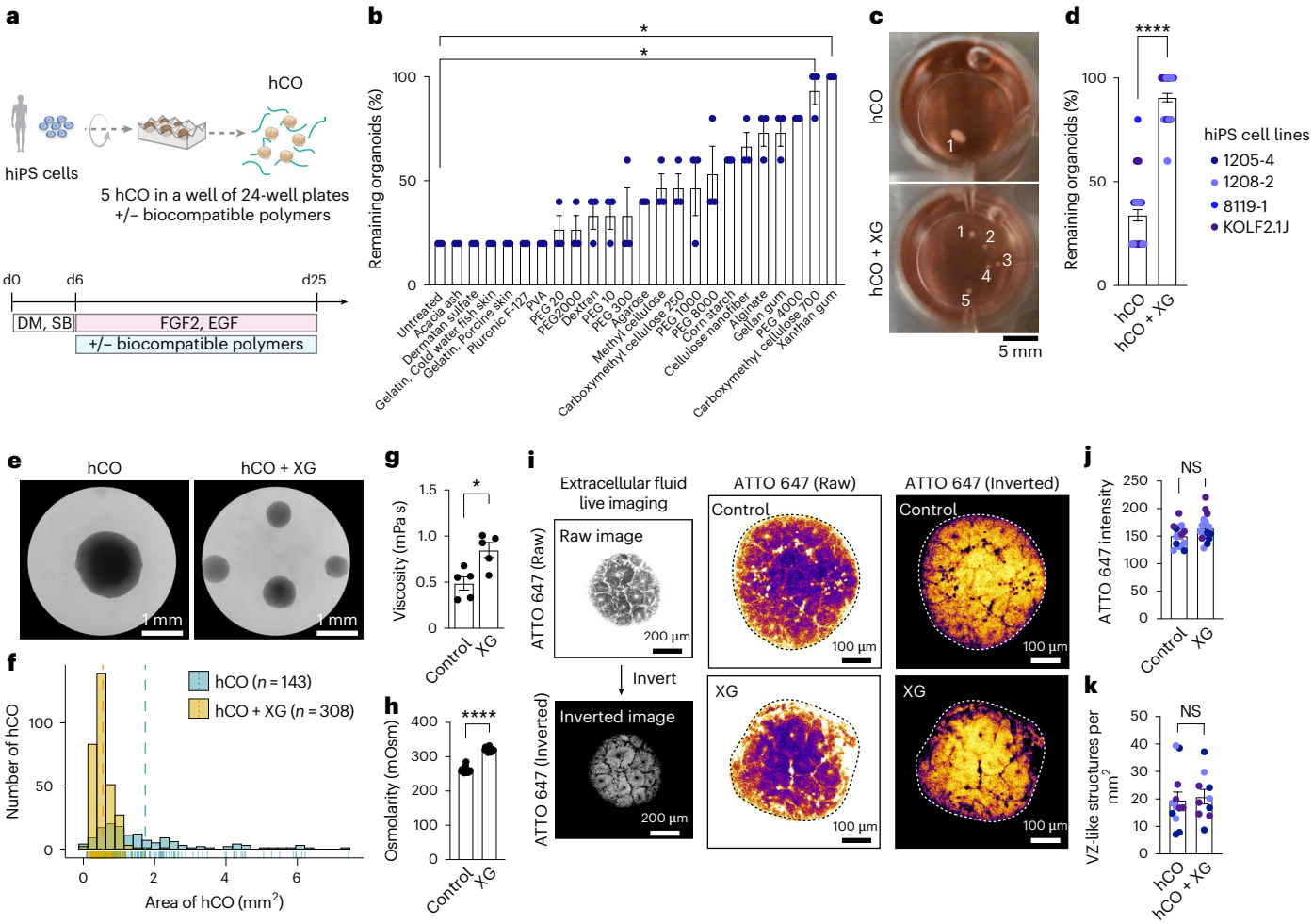

Fig. 1 | Screening of biocompatible polymers for scalable cortical organoid culture. a, Schematic illustrating the screening process of polymers. DM, dorsomorphin; SB, SB431542. **b**, Quantification of remaining organoids of day 25 hCO; $n = 3$ wells for each condition from 1 screening experiment with 1 hiPS cell line. Kruskal–Wallis test, ANOVA result: $^{****}P < 0.0001$, $^{*}P = 0.01$ with multiple comparisons for untreated versus xanthan gum, $^{*}P = 0.03$ for untreated versus carboxymethyl cellulose 700. Data show mean ± s.e.m. **c**, Representative images of untreated hCO (top) and medium with xanthan gum (bottom). **d**, Quantitative graph of remaining organoids; $n = 36$ wells tested for untreated hCO, $n = 36$ wells tested for hCO + XG from 3 differentiation experiments of 4 hiPS cell lines. Two-tailed unpaired *t*-test: $^{****}P < 0.0001$. Data show mean ± s.e.m. **e**, Representative magnified images of untreated hCO and hCO + XG at day 15 of differentiation. **f**, Histogram showing distribution of organoid area at day 15; dashed lines indicate average for each condition. $n = 143$ organoids for untreated hCO, $n = 308$ organoids for hCO + XG from 4 differentiation experiments including 4 hiPS cell lines. **g**, Viscosity measurement of control and XG-supplemented media. $n = 5$ for each condition. Two-tailed unpaired *t*-test: $^{*}P = 0.01$. Data show mean ± s.e.m. **h**, Osmolarity of control and XG-supplemented media. $n = 16$ for control, $n = 14$ for XG-supplemented media. Mann–Whitney test (two-tailed): $^{****}P < 0.0001$. Data show mean ± s.e.m. **i**,**j**, Extracellular fluid live imaging of hCO. Representative raw and inverted images (**i**) and quantification of ATTO 647 intensity (**j**). $n = 15$ organoids for control media, $n = 16$ organoids for XG-supplemented media. Two-tailed unpaired *t*-test: $^{NS}P = 0.08$. Data show mean ± s.e.m. **k**, Density of progenitor ventricular zone (VZ)-like structures. $n = 12$ for hCO, $n = 10$ for hCO + XG. Two-tailed unpaired *t*-test, $^{NS}P = 0.75$. Data show mean ± s.e.m.

food and pharmaceutical formulations[15], significantly reduced spontaneous fusion of hCO compared with the untreated culture medium ($^{*}P = 0.01$ for untreated hCO versus hCO + XG, $^{*}P = 0.03$ for untreated hCO versus carboxymethyl cellulose 700 in Fig. 1b). The effect of XG supplementation was confirmed in cortical organoids differentiated from multiple hiPS cell lines (Fig. 1c and $^{****}P = 0.001$ for Fig. 1d). We also found that XG supplementation yielded hCO of uniform size (Fig. 1e,f), although the degree of fusion slightly depends on hiPS cell lines especially as growth rates can differ in the early stages of neural differentiation[9]. The effect of XG was observed even at a concentration of 0.01% (w/v) XG (Extended Data Fig. 1a). We also tested the XG effect by culturing 5, 10 and 15 organoids in 1 well of a 24-well plate and found that culturing 10 or more organoids can impact efficiency (Extended Data Fig. 1b), which suggests an attenuation of XG anti-fusion effect at high organoid density. Early treatment of XG dramatically reduces organoid fusion without any effects on cortical patterning (Extended Data Fig. 1c–e), which suggests that XG treatment can be started earlier. Supplementation with XG also prevented hCO fusion with higher efficiency than the commercially available STEMdiff Neural Organoid Basal Medium 2 (NOBM), which also prevents organoid fusion ($^{****}P < 0.0001$ for untreated hCO versus hCO + XG, $^{**}P = 0.002$ for hCO + XG versus hCO + STEMdiff NOBM in Extended Data Fig. 2a,b). We noticed no changes in the cortical patterning and cytoarchitecture of NOBM-hCOs and XG-hCOs (Extended Data Fig. 2c–e).

We next investigated the contribution of the biopolymer molecular weight, medium viscosity and medium osmolarity on the XG anti-fusion effect. Medium supplemented with another high molecular weight and negatively charged polymer, hyaluronic acid (HA, M.W. 2,000,000–2,400,000), did not reduce hCO fusion (Extended Data Fig. 3a). This result suggests that the anti-fusion effect of XG is unlikely

https://doi.org/10.1038/s41551-025-01427-3

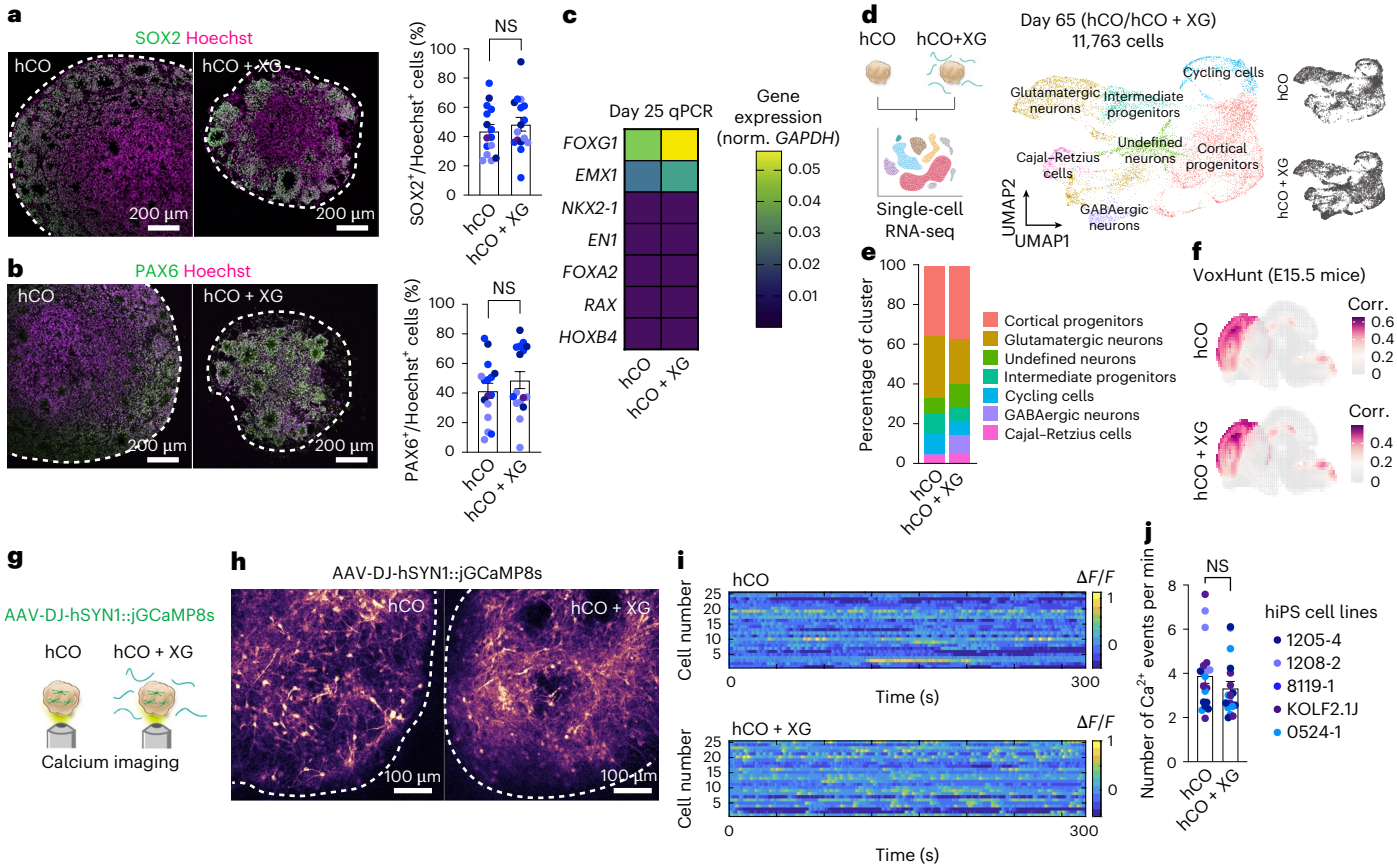

Fig. 2 | Characterization of cortical organoids cultured with XG. **a**, Immunostaining for SOX2 and Hoechst (left), and quantification of SOX2$^+$/Hoechst$^+$ cells (right) in untreated hCO and hCO + XG at day 25. $n = 15$ organoids for untreated hCO, $n = 16$ organoids for hCO + XG from 3 differentiation experiments of 3 hiPS cell lines. Two-tailed unpaired t-test: $^{NS}P = 0.46$. Data show mean ± s.e.m. **b**, Immunostaining for PAX6 and Hoechst (left), and quantification of PAX6$^+$/Hoechst$^+$ cells (right) in untreated hCO and hCO + XG at day 25. $n = 16$ organoids for untreated hCO, $n = 16$ organoids for hCO + XG from 3 differentiation experiments of 3 hiPS cell lines. Two-tailed unpaired t-test: $^{NS}P = 0.35$. Data show mean ± s.e.m. **c**, RT–qPCR of untreated hCO and hCO + XG at day 25; $n = 7$ organoids for untreated hCO, $n = 7$ organoids for hCO + XG from 3 differentiation experiments including 3 hiPS cell lines. Two-tailed Mann–Whitney test: $P = 0.53$ for *FOXG1*, $P = 0.80$ for *EN1*, $P = 0.20$ for *EMX1*, $P = 0.45$ for *NKX2.1*, $P = 0.15$ for *FOXA2*, $P = 0.39$ for *RAX*, $P = 0.45$ for *HOXB4*. Data show mean. **d**, Uniform manifold approximation and projection (UMAP) visualization of single-cell RNA expression in hCO and hCO + XG at day 65 ($n = 5{,}043$ cells for hCO, $n = 6{,}720$ cells for hCO + XG). **e**, Percentage distribution of cell clusters in hCO and hCO + XG conditions. **f**, Unbiased spatial mapping onto the Allen Brain Institute E15.5 mouse brain data using VoxHunt. **g**, Calcium imaging of hCO and hCO + XG neurons expressing jGCaMP8s. **h**, Representative images of cortical organoids expressing jGCaMP8s. **i**, Heatmap showing $\Delta F/F$ of jGCaMP8s signal from 25 cells of hCO and hCO + XG. **j**, Quantification of the number of Ca^{2+} events per min ($n = 19$ cortical organoids (1,959 hCO neurons) and $n = 18$ organoids (2,491 hCO + XG neurons) with 4 hiPS cell lines from 3 differentiations); two-tailed Mann–Whitney test: $^{NS}P = 0.19$. Data show mean ± s.e.m.

to be attributed just to the biopolymer molecular weight. XG supplementation led to increased viscosity ($^*P = 0.01$ for Fig. 1g) and osmolarity ($^{****}P < 0.0001$ for Fig. 1h) of the medium, suggesting that changes in these biophysical properties may contribute to the anti-fusion effect. To test whether these changes interfere with medium penetration into hCO, we performed extracellular fluid imaging[16] by supplementing with a fluorescent dye (Fig. 1i). We found that XG medium penetrates well within hCO as compared with XG-free medium (Fig. 1i,j).

We explored changes in organoid size and cell composition following XG supplementation during neural differentiation. We found that the cross-sectional area of XG-hCO was smaller than in the untreated condition ($P = 0.99$ for day 3, $^{****}P < 0.0001$ for day 10, $^{****}P < 0.0001$ for day 15 for Extended Data Fig. 3b). To verify whether this is due to prevention of fusion rather than just interference with organoid growth, we individually cultured organoids in XG or XG-free media in single wells of low attachment cell culture plates. We then compared organoid size between untreated hCO and XG-treated hCO at day 15 and found that XG treatment did not impair organoid growth; in fact, there was a slight increase in hCO size, potentially due to positive effects of XG treatment on hCO growth (Extended Data Fig. 3c). This indicates that the size reduction shown in Extended Data Fig. 3b is probably related to prevention of fusion by XG. To further investigate the potential impact of XG on neural differentiation, we inspected their cytoarchitecture by immunocytochemistry. XG-treated hCO displayed a comparable number of ventricular zone-like structures containing SOX2$^+$ cells in individual and bulk-culture conditions (Figs. 1k and 2a,b and Extended Data Fig. 4a,b). The percentage of neural progenitor (SOX2$^+$) cells (Fig. 2a, $P = 0.72$) and dorsal forebrain progenitor (PAX6$^+$) cells (Fig. 2b, $P = 0.66$) were comparable to the untreated hCO condition. The percentage of PAX6$^+$ cells is slightly lower when organoids are cultured individually than when cultured in the same plate (Fig. 2b and Extended Data Fig. 4b). This could be related to differences in the induction of PAX6 at different cell densities, as previously shown[17]. XG neither induced cytotoxicity as measured by an LDH cytotoxicity assay ($P = 0.48$ for Extended Data Fig. 4c), nor induced expression of the apoptotic cell death marker cleaved caspase-3 (Extended Data Fig. 4d). In addition, hCO cultured with XG did not display differences in the expression of the forebrain marker *FOXG1* ($P = 0.53$ in Fig. 2c, $P = 0.54$

https://doi.org/10.1038/s41551-025-01427-3

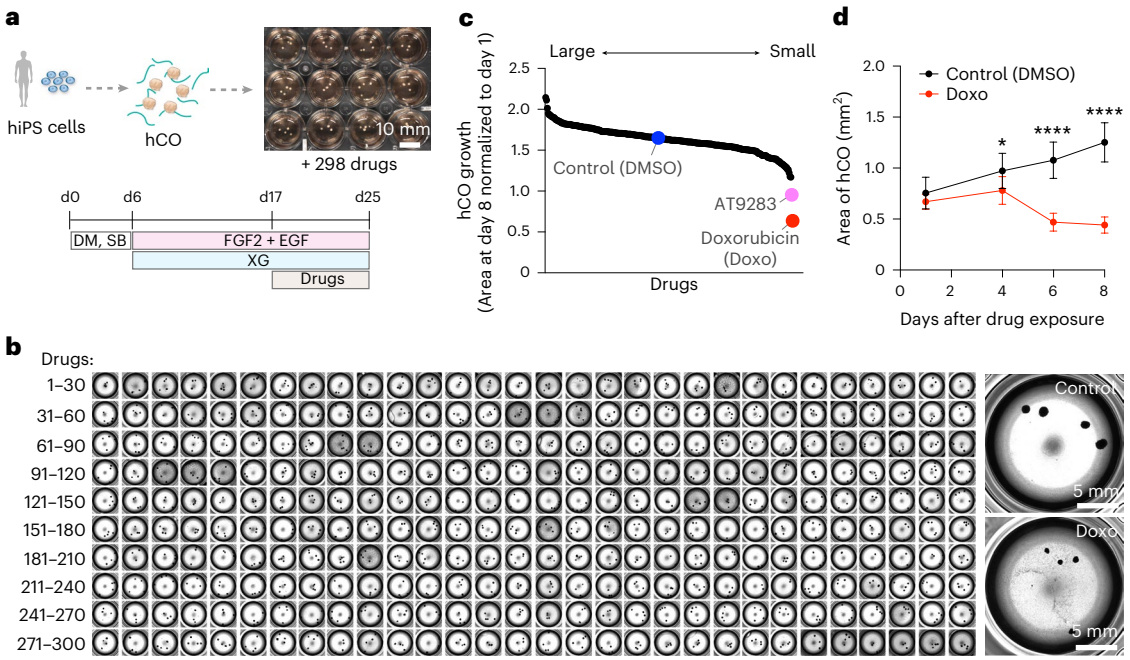

Fig. 3 | Effects of 298 FDA-approved drugs and teratogens on cortical organoids. a, Schematic showing the screening of 298 drugs in hCO. **b**, Images of hCO treated with 298 drugs for 8 days. Top right: control; bottom right: doxorubicin (Doxo). **c**, Quantification of size of organoid treated with drugs. Data show mean. **d**, Area of control hCO or hCO treated with Doxo for 8 days; $n = 8$ organoids (control hCO), $n = 9$ organoids (days 1, 4) and $n = 8$ organoids (days 6, 8) of Doxo-treated hCO from 1 screening experiment of 1 hiPS cell line. Two-way ANOVA: $^{****}P < 0.0001$, $^{*}P = 0.02$ (day 4), $^{****}P < 0.0001$ (days 6, 8) with Šidák multiple comparisons test. Data show mean ± s.d.

in Extended Data Fig. 4e) or the dorsal cortical marker *EMX1* ($P = 0.20$ in Fig. 2c, $P = 0.84$ in Extended Data Fig. 4e), and lacked expression of the midbrain marker *EN1* ($P = 0.80$ in Fig. 2c, $P > 0.9999$ in Extended Data Fig. 4e), the medial ganglionic eminence marker *NKX2-1* ($P = 0.45$ in Fig. 2c, $P = 0.69$ in Extended Data Fig. 4e), the floor plate marker *FOXA2* ($P = 0.15$ in Fig. 2c, $P = 0.69$ in Extended Data Fig. 4e), the hypothalamic marker *RAX* ($P = 0.39$ in Fig. 2c, $P = 0.16$ in Extended Data Fig. 4e), or the hindbrain/spinal cord marker *HOXB4* ($P = 0.45$ in Fig. 2c, $P = 0.55$ in Extended Data Fig. 4e). We next carried out several experiments at later stages (up to 14 weeks) of hCO differentiation. First, we performed single-cell RNA sequencing (scRNA-seq) analysis on day 65 hCO and hCO + XG (Fig. 2d,e), which revealed no major changes in forebrain identity following XG treatment. Unbiased spatial mapping using VoxHunt further confirmed that the overall patterning was comparable between the two conditions (Fig. 2f). Both conditions included cortical glutamatergic neurons (*TBR1*$^{+}$), cortical progenitors (*PAX6*$^{+}$) and cycling cells (*MKI67*$^{+}$) (Fig. 2d,e and Extended Data Fig. 5a–d). Astrocyte markers are present after 100–150 days in cultures[18]; hCO + XG had slightly more GABAergic neurons, which is still in range of the amount and differences reported in previous hCO scRNA-seq data[13,19], and there are no noticeable expressions of markers for ventral forebrain (*DLX2*), lateral ganglionic eminence (*GSX2*) and medial ganglionic eminence (*NKX2-1*) (Extended Data Fig. 5a). We also found a cluster of undefined neurons, which express the pan-neuronal marker, *STMN2*, but none of the classic neurotransmitters identify markers, such as glutamatergic neuron markers (*SLC17A7*, *SLC17A6*) or GABAergic neuron markers (*GAD1*) (Extended Data Fig. 5a). These cells could be related to the maturation of neurons to obtain a clear neuronal identity, although they seem not to affect neuronal specification or maturation[20,21]. The correlation of normalized gene expression between the two conditions was $R^2 = 0.986$ ($^{****}P < 0.001$) (Extended Data Fig. 5c). Immunocytochemistry experiments showed the presence of the deep layer marker CTIP2 at day 62, as well as expression of glial-lineage marker GFAP and the upper layer marker SATB2 at day 100 (Extended Data Fig. 6a). We analysed the effects of XG supplementation on the morphological development of neurons in cortical organoids by 3D live confocal imaging of eYFP expressing neurons and found no significant changes in soma area, soma circularity and the number of neurites (Extended Data Fig. 6b). To further investigate whether XG treatment affects neuronal activity in hCO, we infected hCO and XG-hCO with adeno-associated virus (AAV) expressing genetically encoded calcium indicator jGCaMP8s[22] under human synapsin promoter and analysed the numbers of calcium events (Fig. 2g,h). We found that the neuronal activity of organoids grown with XG was comparable to the control culture condition (Fig. 2i,j). Taken together, these data indicate that patterning, differentiation and maturation of neurons in hCO are not adversely affected by the presence of XG in the culture medium.

We next verified whether XG enables large-scale culture and screening of hCO. Teratogenic risk has not been established for the great majority of FDA-approved drugs primarily because pregnant women are not generally included in clinical trials[23]. There is a great need for human models to assess the potential risk of neuropsychiatric or cancer drugs during pregnancy. Towards this end and to leverage the scalability of the XG-hCO, we tested the effect of a group of FDA-approved drugs on in vitro cortical development. We compiled a list of 298 drugs that includes FDA-approved compounds for neuropsychiatric conditions and a group of teratogens[24]. We then cultured multiple hCO per well in several 24-well plates with XG-supplemented media, and tested the effect of 1 µM of each of the 298 FDA-approved drugs (Supplementary Table 4), with DMSO treatment alone as a control, from day 17 to 25 of differentiation (Fig. 3a). Due to the anti-fusion effect of XG, one researcher was able to differentiate and maintain over 2,000 organoids at the same time. To assess the acute effects of drugs on morphological changes of hCO, we imaged and analysed the area of hCO at 8 days after drug exposure and found that several compounds affect the size of hCO (Fig. 3b,c and Supplementary Table 5). In particular, doxorubicin (Doxo), a breast cancer drug with known teratogen properties[24,25], significantly reduced the size of hCO at 6 days

https://doi.org/10.1038/s41551-025-01427-3

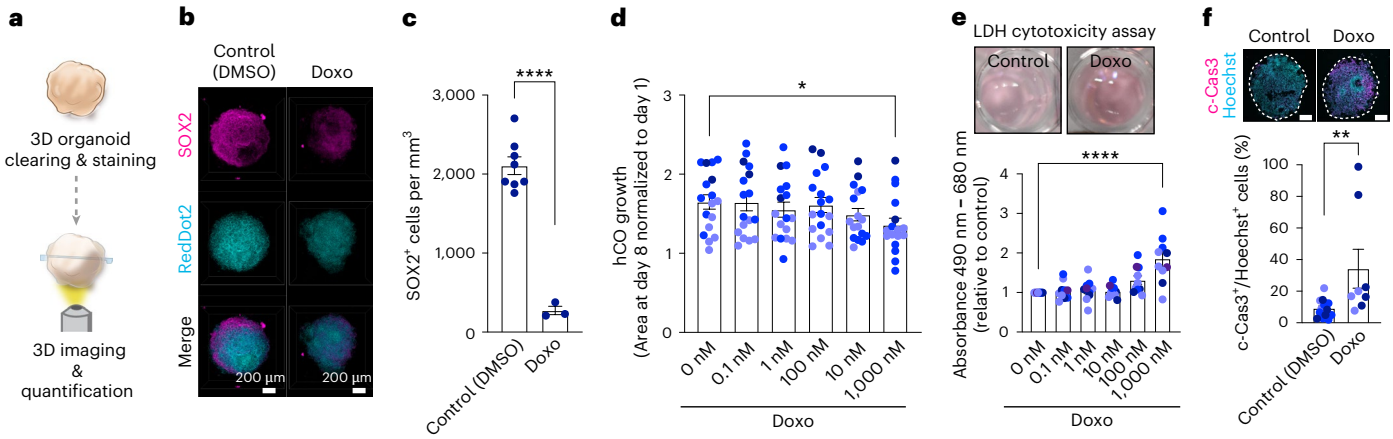

Fig. 4 | Effects of doxorubicin on cortical organoids. a, Schematic illustrating 3D clearing and staining of control and Doxo-treated hCO. **b**, 3D immunostaining of CUBIC-cleared hCO cultured with Doxo or control. **c**, Quantification of SOX2$^+$ cells in 3D-cleared hCO treated with Doxo or control; $n = 8$ organoids for control hCO; $n = 3$ organoids for Doxo-treated hCO from 1 screening experiment of 1 hiPS cell line. Two-tailed unpaired t-test: $^{****}P < 0.0001$. Data show mean ± s.e.m. **d**, Organoid growth ratio of hCO treated with or without Doxo for 8 days; $n = 17$ organoids for each condition from 3 differentiation experiments of 4 hiPS cell lines. One-way ANOVA: $^{*}P = 0.01$, $P > 0.9999$ with Tukey's multiple comparisons test for 0 nM versus 0.1 nM, $P = 0.90$ for 0 nM versus 1 nM, $P = 0.99$ for 0 nM versus 10 nM, $P = 0.53$ for 0 nM versus 100 nM, $^{*}P = 0.02$ for 0 nM versus 1,000 nM. Data show mean ± s.e.m. **e**, LDH cytotoxicity assay at day 25 of hCO treated for 8 days with 1 µM of Doxo. Images are for control (top left) and Doxo (top right) treatments; $n = 10$ wells for each condition from 3 differentiation experiments of 4 hiPS cell lines. One-way ANOVA: $^{****}P < 0.0001$, $P = 0.99$ with Dunnett's multiple comparisons test for 0 nM versus 0.1 nM, $P = 0.99$ for 0 nM versus 1 nM, $P = 0.99$ for 0 nM versus 10 nM, $P = 0.13$ for 0 nM versus 100 nM, $^{****}P < 0.0001$ for 0 nM versus 1,000 nM. Data show mean ± s.e.m. **f**, Top: immunostaining for cleaved caspase-3 (c-Cas3) (magenta) and Hoechst (cyan) in control hCO or hCO treated with Doxo for 8 days at day 25. Bottom: quantification of c-Cas3$^+$/Hoechst$^+$ cells; $n = 14$ organoids for control hCO, $n = 8$ organoids for Doxo-treated hCO from 2 differentiation experiments including 3 hiPS cell lines. Scale bars, 200 µm. Two-tailed Mann–Whitney test: $^{**}P = 0.0064$. Data show mean ± s.e.m.

post exposure ($^{*}P = 0.02$ for day 4, $^{****}P < 0.0001$ for days 6 and 8 for Fig. 3d). CUBIC clearing combined with 3D staining of hCO (Fig. 4a) confirmed a lower density of SOX2$^+$ cells in hCO treated with Doxo (Fig. 4b and $^{****}P < 0.0001$ for Fig. 4c). We verified this effect using a different batch of Doxo and in multiple hiPS cell lines, and again found growth impairment in Doxo-treated hCO ($^{*}P = 0.02$ for Fig. 4d and Extended Data Fig. 7a–c), as well as increased cytotoxicity in an LDH cytotoxicity assay ($^{****}P < 0.0001$ for Fig. 4e), both of which present dose-dependent effects. Furthermore, we found increased expression of the apoptotic cell marker cleaved caspase-3 ($^{**}P = 0.006$ for Fig. 4f), which suggests that Doxo may cause cell death of cortical cells or impair the proliferation of progenitors. We also investigated an additional screen hit, AT9283, a JAK2/3 inhibitor that reduces hCO area (Fig. 3c), and found dose-dependent effects on organoid growth (Fig. 5a,b) and cytotoxicity (Fig. 5c). Furthermore, we discovered that AT9283 treatment is associated with a reduced number of SOX2$^+$ cells (Fig. 5d).

Discussion

In this study, we describe an improvement to a neural organoid culture approach we have previously developed. This is achieved by the simple application of an inexpensive, biocompatible polymer that reduces spontaneous fusions of organoids and thereby enables one single researcher to differentiate and maintain thousands of organoids in parallel. We highlight the advantage of culturing multiple organoids in larger plates in the presence of XG over individually growing organoids in single wells, which can effectively scale production and maintenance while reducing both maintenance time and cell culture media costs. This approach could facilitate screens even in laboratories with a limited budget. Other biocompatible polymers, such as the anionic polysaccharide gellan gum, can also be used to enable screening in assembloids[26]. Some of the commercially available media may contain polymers, but the lack of information on chemical composition[27] often poses challenges for direct comparison across media. Although we explored the effects of XG supplementation and detected no significant changes in cortical patterning, differentiation, morphological development and neural activity of neurons in cortical organoids, differences in other parameters and at specific times of differentiation may be triggered by XG supplementation. As a proof of concept, we leveraged this platform to examine the effect of several hundred drugs on neural organoid growth and identified a previously known teratogen compound as potentially being cytotoxic to neural cells. The approach is also compatible with bioreactor systems or can be combined with automated culture methods that employ bulk media changes with liquid handlers or robotic arms to further increase scalability. Combining this with high-content imaging, such as calcium imaging[28,29], can further increase the scale of screen readouts. In principle, this polymer can be used for generating other regionalized neural and non-neural organoids. Taken together, we envision that this simple differentiation approach could substantially increase the applications of organoids, especially at the early stage of cortical development for large-scale disease modelling and compound screening.

Methods

Characterization and maintenance of hiPS cells

Human induced pluripotent stem cell lines were validated using standardized methods as described previously[9,30,31]. Cultures were tested for and maintained *Mycoplasma* free. A total of 5 control hiPS cell lines were used. KOLF2.1J hiPS cell line was obtained from the Jackson Laboratory[32]. Approval for this study was obtained from the Stanford Institutional Review Board (IRB) panel and informed consent was obtained from all participants. For maintenance of hiPS cells, the cells were cultured on vitronectin-coated plates (5 µg ml^{-1}, Thermo Fisher, A14700) in Essential 8 medium (Thermo Fisher, A1517001). Cells were passaged every 4 or 5 days with UltraPure 0.5 mM EDTA, pH 8.0 (Thermo Fisher, 15575020).

Generation of hCO from hiPS cells

For the generation of hCO, hiPS cells were incubated with Accutase (Innovative Cell Technologies, AT104) at 37 °C for 7–10 min and dissociated into single cells. Optionally, 1–2 days before spheroid formation,

https://doi.org/10.1038/s41551-025-01427-3

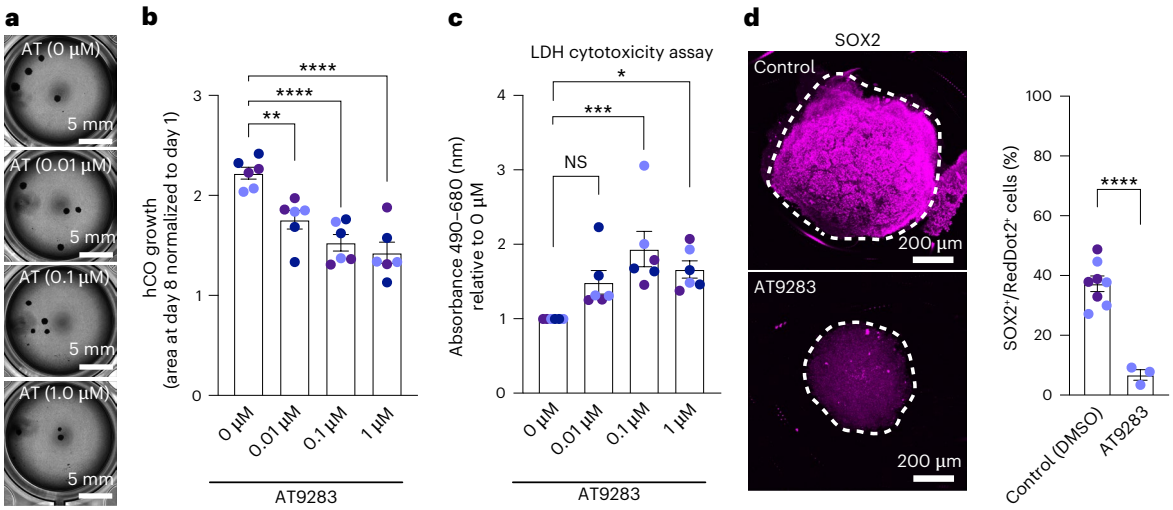

Fig. 5 | Effects of AT9283 on cortical organoids. a,**b**, Representative images (**a**) and quantitative data (**b**) of control hCO and AT-treated hCO. $n = 6$ organoids for each condition; one-way ANOVA: $F = 0.2377_{(3,20)}$, $^{****}P < 0.0001$, $^{**}P = 0.005$ with Tukey's multiple comparisons test for control versus AT 0.01 µM, $^{****}P < 0.0001$ for control versus AT 0.1 µM, $^{****}P < 0.0001$ for control versus AT 1 µM. **c**, LDH cytotoxicity assay of day 25 hCO and AT-treated hCO; $n = 6$ wells for each condition. One-way ANOVA: $F = 1.257_{(3,20)}$, $^{NS}P = 0.08$ with Dunnett's multiple comparisons test for control versus AT 0.01 µM, $^{***}P = 0.0009$ for control versus AT 0.1 µM, $^{*}P = 0.0161$ for control versus AT 1 µM. **d**, Left: 3D immunostaining of CUBIC-cleared hCO cultured with AT9283 (1 µM). Right: quantification of SOX2^{+} cells in 3D-cleared hCO treated with AT9283; $n = 8$ organoids for control hCO; $n = 3$ organoids for AT9283-treated hCO (2 hiPS cell lines). Two-tailed unpaired *t*-test: $^{****}P < 0.0001$. Data show mean ± s.e.m.

hiPS cells could be exposed to 1% dimethylsulfoxide (DMSO) (MilliporeSigma, D2650) in Essential 8 medium. To obtain uniformly sized spheroids, AggreWell-800 culture plates (STEMCELL Technologies, 34815) containing 300 microwells were used. Approximately 2×10^6 single cells were added per AggreWell-800 well in Essential 8 medium supplemented with the ROCK inhibitor Y-27632 (10 µM, Selleckchem, S1049), centrifuged at 100 *g* for 3 min to capture the cells in the microwells and incubated at 37 °C with 5% CO_2. After 24 h, organoids consisting of ~6,666 cells were collected from each microwell by pipetting medium in the well up and down with a cut P1000 pipet tip and transferred into ultra-low attachment plastic dishes (Corning, 3262) in Essential 6 medium (Thermo Fisher, A1516401) supplemented with two SMAD pathway inhibitors: dorsomorphin (2.5 µM, Sigma-Aldrich, P5499) and SB-431542 (10 µM, R&D Systems, 1614). On day 6 in suspension, the organoids were transferred to neural medium containing Neurobasal-A medium (Thermo Fisher, 10888022), B-27 Supplement minus vitamin A (Thermo Fisher, 12587010), GlutaMAX Supplement (1:100, Thermo Fisher, 35050079), penicillin–streptomycin (1:100, Thermo Fisher, 15070063), and supplemented with 20 ng ml^{-1} EGF (R&D Systems, 236-EG) and 20 ng ml^{-1} FGF2 (R&D Systems, 233-FB). From day 15 of differentiation, media were changed every other day. From day 25, to promote differentiation of the neural progenitors into neurons, the neural medium was supplemented with brain-derived neurotrophic factor (BDNF; 20 ng ml^{-1}, PeproTech, 450-02) and NT3 (20 ng ml^{-1}, PeproTech, 450-03). From day 45, only neural medium containing B-27 Supplement minus vitamin A (Thermo Fisher, 12587010) was used for medium changes every 4 days.

Screening of biocompatible polymers to prevent hCO fusion

At day 6 of differentiation, 5 hCO were transferred into 1 well of a 24-well plate containing culture media with 0.1% (w/v) of polymers (Supplementary Table 1). At day 25, the remaining organoids in each well were imaged using REVOLVE microscope (ECHO), and their numbers were counted. When XG was not present in the culture media, we did not manually separate the organoids between days 0 and 6, as well as after day 25. For comparison to hCO cultured in STEMdiff Neural Organoid Basal Medium 2 (hCO + STEMdiff NOBM, STEMCELL Technologies, 08620), the remaining organoids in each well were imaged at day 12 on a REVOLVE microscope (ECHO) or a BZX-710 (KEYENCE) with ×4 lens. To prepare the XG-supplemented media, the XG powder, which was difficult to dissolve, was mixed with 100% ethanol. More specifically, to make 250 ml of XG-supplemented Neurobasal medium (0.2% XG [w/v], which is a 2× stock solution), 0.5 *g* of XG powder was mixed with 2 ml of 100% ethanol, and 248 ml of Neurobasal medium was then immediately added on top and mixed to avoid the formation of XG clumps. To avoid contamination, dedicated equipment was used inside a biosafety cabinet to weigh XG and mix the medium.

Characterization of media properties

A Rheosense m-VROC viscometer (m-VROC software v.3.1.5) was used to collect viscosity data. Samples were loaded into a 1 ml Hamilton syringe and viscosity was measured at a steady state under high shear rate to maximize pressure signal. The osmolarity of the medium was measured using a 5010 OSMETTE III Fully Automatic 10 µl osmometer (Precision Systems).

Extracellular fluid imaging

ATTO 647 (ATTO-TEC, AD 647-21) was used for extracellular fluid imaging. hCO were incubated with 50 µM of ATTO 647 in culture media with or without XG for 30 min and imaged using a ×10 objective on a Leica TCS SP8 confocal microscope. Images were processed and quantified with ImageJ/Fiji (v.2.3.0/1.53f, NIH).

Cryoprotection and immunocytochemistry

hCO were fixed in 4% paraformaldehyde (PFA)/phosphate buffered saline (PBS) overnight at 4 °C. Next day, they were washed in PBS and transferred to 30% sucrose/PBS for 2–3 days until the spheres sank in the solution. Subsequently, they were rinsed in optimal cutting temperature (OCT) compound (Tissue-Tek OCT Compound 4583, Sakura Finetek) and 30% sucrose/PBS (1:1), and embedded. For immunofluorescence staining, 10- or 20-µm-thick sections were cut using a Leica Cryostat (Leica, CM1860). Cryosections were washed with PBS to remove excess OCT on the sections and blocked in 10% Normal Donkey Serum (NDS, Abcam, ab7475), 0.3% Triton X-100 (MilliporeSigma, T9284-100ML) and 0.1% BSA diluted in PBS (or without NDS) for 1 h at room temperature. The sections were then incubated overnight at 4 °C with

primary antibodies diluted in PBS containing 2% NDS and 0.1% Triton X-100 (or without NDS). PBS was used to wash the primary antibodies and the cryosections were incubated with secondary antibodies in PBS, with the PBS containing 2% NDS and 0.1% Triton X-100 (or without NDS) for 1 h. The following primary antibodies were used for staining: anti-SOX2 (rabbit, Cell Signaling Technology, 3579, 1:300 dilution), anti-PAX6 (mouse, DSHB, PAX6, 1:50 dilution), anti-cleaved caspase-3 (Asp175) (rabbit, Cell Signaling Technology, 9661, 1:200 dilution), FITC anti-CTIP2 antibody [25B6] (rat, Abcam, ab123449, 1:100 dilution), anti-GFAP (rabbit, DAKO, Z0334, 1:1,000 dilution), anti-MAP2 (guinea pig, Synaptic Systems, 188 004, 1:200 dilution) and anti-SATB2 (mouse, Abcam, ab51502, 1:50 dilution). Alexa Fluor dyes, donkey anti-rabbit IgG (H&L) highly cross-adsorbed secondary antibody, Alexa Fluor 488 (Thermo Fisher, A-21206), donkey anti-mouse IgG (H&L) highly cross-adsorbed secondary antibody, Alexa Fluor 568 (Thermo Fisher, A10037, 2110843) and Alexa Fluor 647 AffiniPure donkey anti-guinea pig IgG (H + L) (Jackson ImmunoResearch, 706-605-148) were used at 1:500–1:1,000 dilution, and nuclei were visualized with Hoechst 33258 (Thermo Fisher Scientific, H3569, 1:10,000 dilution). Cryosections were mounted for microscopy on glass slides using Aquamount medium (Polysciences, 18606) and imaged on a Leica TCS SP8 or Stellaris 5 confocal microscope. Images were processed in ImageJ/Fiji (v.2.3.0/1.53f, NIH) and quantified using Imaris (Oxford Instruments, v.9.6)., 2110843) and Alexa Fluor 647 AffiniPure donkey anti-guinea pig IgG (H + L) (Jackson ImmunoResearch, 706-605-148) were used at 1:500–1:1,000 dilution, and nuclei were visualized with Hoechst 33258 (Life Technologies, H3549, 10,000 dilution). Cryosections were mounted for microscopy on glass slides using Aquamount medium (Polysciences, 18606) and imaged on a Leica TCS SP8 or Stellaris 5 confocal microscope. Images were processed in ImageJ/Fiji (v.2.3.0/1.53f, NIH) and quantified using Imaris (Oxford Instruments, v.9.6).

Reverse transcription–quantitative PCR

mRNA from hCO and hCO + XG at day 25 were isolated using the RNeasy Mini kit (Qiagen, 74106) with DNase I, amplification grade (Thermo Fisher, 18068-015). Template complementary DNA was prepared by reverse transcription using the SuperScript III First-Strand Synthesis SuperMix for RT–qPCR (Thermo Fisher, 11752250). RT–qPCR was performed using the SYBR Green PCR Master Mix (Thermo Fisher, 4312704) on a QuantStudio 6 Flex Real-Time PCR System (Thermo Fisher, 4485689). Primers used in this study are listed in Supplementary Table 2.

Single-cell dissociation, sample preparation for scRNA-seq and data analysis

Dissociation of hCO was performed as previously described[7]. Randomly selected 4–6 organoids were pooled to obtain a single cell suspension and then incubated in a 30 U ml^{-1} papain enzyme solution (Worthington Biochemical, LS003126) with 0.4% DNase (12,500 U ml^{-1}, Worthington Biochemical, LS2007) for 45 min at 37 °C. After enzymatic dissociation, organoids were washed with a trypsin inhibitor and gently triturated to obtain a single cell suspension. Cells were then resuspended in 0.04% BSA/PBS (MilliporeSigma, B6917-25MG) and filtered through a 70 µm Flowmi Cell Strainer (Bel-Art, H13680-0070). The number of cells was counted using a Countess 3 FL Automated Cell Counter (Thermo Fisher, AMQAF2000). To target 7,000 cells after recovery, ~11,600 cells were loaded per lane on a Chromium Single Cell 3′ chip (Chromium Next GEM Chip G Single Cell Kit, 10x Genomics, PN-1000127). cDNA libraries for samples were prepared with the Chromium Next GEM Single Cell 3′ GEM, Library & Gel Bead Kit v.3.1 (10x Genomics, PN-1000128) according to manufacturer instructions. Each library sample was sequenced using the Illumina NovaSeq 6000 S4 system, 2 × 150 bp by Admera Health. Quality control, unique molecular identifiers (UMI) counting of Ensembl genes and aggregation of samples were performed by the 'count' and 'aggr' functions using Cell Ranger software (Cellranger v.6.0.1) on the 10X cloud platform. Further downstream analyses were performed using the R package Seurat (v.4.1.2). Genes that were not expressed in at least three cells were not included in the analysis. Cells with more than 10,000 or less than 500 detected genes or with mitochondrial content higher than 10% were excluded. Gene expression was normalized using a global-scaling normalization method (normalization method, 'LogNormalize'; scale factor, 10,000), and the 2,000 most variable genes were selected (selection method, 'vst') and scaled before principal component analysis. The top 15 principal components were applied for clustering (resolution of 0.4), using the 'FindNeighbors' and 'FindClusters' functions, and for visualization with uniform manifold approximation and projection (UMAP). Clusters were grouped on the basis of the expression of known marker genes (Extended Data Fig. 5a,b). The FindAllMarkers function with a Wilcoxon Rank Sum test (two-sided) was used to identify differentially expressed genes per cluster (Supplementary Table 3). Unbiased spatial mapping of each sample was performed using VoxHunt[33] (VoxHunt v.1.0.0); the 150 most variable features from the ISH Allen Brain Atlas data of the E15.5 mouse brain were selected, and similarities to the atlas data were calculated. These maps were then plotted in the sagittal views of the mouse brain.

Testing effects of drugs on hCO

At day 17 of differentiation, multiple hCO were transferred into 1 well of a 24-well plate containing neurobasal media with xanthan gum. These hCO were treated with 1 µM of FDA-approved drugs or teratogens dissolved in DMSO or water (Supplementary Table 4), or only DMSO was used as a control. Drugs were applied every other day during medium change. At 1, 4, 6 and 8 days after drug treatment, all hCO in individual wells were imaged using a BZX-710 microscope (KEYENCE) with ×4 lens, and the area of each sphere was quantified using imageJ/Fiji (v.2.3.0/1.53f, NIH). Organoids that were fused in the wells were excluded from the analysis, and the mean area normalized to the area of hCO on day 1 was calculated to reduce the impact of any potential size difference at the start of the experiment.

LDH cytotoxicity assay

At day 25 of hCO culture, 50 µl of culture media from individual wells of culture well plates were collected and the LDH cytotoxicity assay was performed using CyQUANT LDH Cytotoxicity Assay (Thermo Fisher, C20300) following company instruction.

Clearing and 3D staining of hCO

To optically clear and image hCO, we applied the hydrophilic chemical cocktail-based CUBIC protocol[34]. hCO at day 25 were fixed with a 4% PFA/PBS solution at 4 °C overnight. The next day, samples were washed twice with PBS and incubated in Tissue-Clearing Reagent CUBIC-L (TCI, T3740) at 37 °C for 2 d. Samples were washed three times with PBS, then nuclear staining was performed with RedDot2 (Biotium, 40061, 1:150 dilution) in PBS containing 500 mM NaCl at 37 °C overnight. Samples were washed twice with PBS and once with a solution containing 10 mM HEPES, 10% Triton X-100, 200 mM NaCl and 0.5% BSA (HEPES-TSB) at 37 °C for 2 h, and then stained with anti-SOX2 (rabbit, Cell Signaling Technology, 3579, 1:100 dilution) antibody in HEPES-TSB solution at 37 °C for 2 d. Stained spheres were subsequently washed twice with 10% Triton X-100 in PBS and once with HEPES-TSB solution for 2 h each, and then incubated with donkey anti-rabbit IgG (H&L) highly cross-adsorbed secondary antibody and Alexa Fluor 488 (Thermo Fisher, A-21206, 1:300 dilution) in HEPES-TSB solution at 37 °C for 2 d. Samples were washed twice with 10% Triton X-100 in PBS for 30 min and once with PBS for 1 h. After washing with PBS, samples were incubated with Tissue-Clearing Reagent CUBIC-R+ (TCI, T3741) at room temperature for 2 d for refractive index matching. CUBIC-cleared hCO were then transferred into a well of a Corning 96-well microplate (Corning, 4580) in 150 µl of CUBIC-R+ solution and imaged using a ×10 objective on a Leica TCS SP8 confocal microscope.

Viral labelling and imaging

Viral labelling and imaging of organoids were performed as previously described[30,31]. hCO (~day 60) were transferred into a 1.5 ml Eppendorf tube containing 200 µl of neural media with 0.5 µl of AAV and incubated overnight at 37 °C and 5% CO_2. The next day, 800 µl of fresh neural medium was supplemented. The following day, hCO were transferred into fresh neural media in ultra-low attachment plates (Corning, 3471, 3261). For live-cell imaging, virally labelled hCO were transferred into a 20 mm glass coverslip in a 35 mm glass-bottom well (Cellvis, D35-20-0-N) and incubated in an environmentally controlled chamber for 15–30 min before imaging on a Leica Stellaris 5 confocal microscope. Images were processed in ImageJ/Fiji (v.2.3.0/1.53f, NIH). The viruses used in this study were: AAV-DJ-hSYN1::eYFP (Stanford University Neuroscience Gene Vector and Virus Core, GVVC-AAV-16) and hSYN1-jGCaMP8s-WPRE (Stanford University Neuroscience Gene Vector and Virus Core, GVVC-AAV-230).

Calcium imaging and analysis

Cortical organoids expressing jGCaMP8s were transferred into a 24-well glass-bottom plate (Cellvis, P24-0-N) and incubated in an environmentally controlled chamber for 15–30 min before calcium imaging on a Leica Stellaris 5 confocal microscope. Organoids were imaged using a ×10 objective at a frame rate of 5 frames per second, and results were analysed with ImageJ/Fiji (v.2.3.0/1.53f, NIH), Python and MATLAB (v.9.13.0.2105380, R2022b, MathWorks). More specifically, TIFF files were exported from original raw files (lif files) and GaussianBlur3D was used for filtration with ImageJ/Fiji (v.2.3.0/1.53f, NIH). Suite2p was used to automatically detect regions of interest. After $\Delta F/F_0$ values were calculated from raw signals, a custom code using a slope-change-based method with a threshold based on standard deviation (percentile_value = 40, threshold_factor = 2, min_threshold = 0.15) was implemented to obtain the number of Ca^{2+} events in active neurons.

Statistics

Data are presented as mean ± s.e.m., mean ± s.d., or only mean value. Raw data were tested for normality of distribution, and statistical analyses were performed using an unpaired *t*-test (two-tailed) or one-way analysis of variance (ANOVA) with multiple comparison tests. Sample sizes were estimated empirically. GraphPad Prism v.9.3.1 was used for statistical analyses.

Reporting summary

Further information on research design is available in the Nature Portfolio Reporting Summary linked to this article.

Data availability

Gene expression data have been deposited in the Gene Expression Omnibus (GEO) under accession number GSE232581 (ref. 35). The data in this study are provided in the Source Data files and available on request from the corresponding author. Source data are provided with this paper.

Code availability

The custom code used for calcium imaging analysis has been deposited on Zenodo at https://doi.org/10.5281/zenodo.15092416 (ref. 36).

References

1. Qian, X., Song, H. & Ming, G. L. Brain organoids: advances, applications and challenges. *Development* **146**, dev166074 (2019).
2. Chiaradia, I. & Lancaster, M. A. Brain organoids for the study of human neurobiology at the interface of in vitro and in vivo. *Nat. Neurosci.* **23**, 1496–1508 (2020).
3. Kelley, K. W. & Pasca, S. P. Human brain organogenesis: toward a cellular understanding of development and disease. *Cell* **185**, 42–61 (2022).
4. Hofer, M. & Lutolf, M. P. Engineering organoids. *Nat. Rev. Mater.* **6**, 402–420 (2021).
5. Roth, J. G. et al. Advancing models of neural development with biomaterials. *Nat. Rev. Neurosci.* **22**, 593–615 (2021).
6. Pasca, A. M. et al. Functional cortical neurons and astrocytes from human pluripotent stem cells in 3D culture. *Nat. Methods* **12**, 671–678 (2015).
7. Sloan, S. A., Andersen, J., Pasca, A. M., Birey, F. & Pasca, S. P. Generation and assembly of human brain region-specific three-dimensional cultures. *Nat. Protoc.* **13**, 2062–2085 (2018).
8. Trevino, A. E. et al. Chromatin accessibility dynamics in a model of human forebrain development. *Science* **367**, eaay1645 (2020).
9. Yoon, S. J. et al. Reliability of human cortical organoid generation. *Nat. Methods* **16**, 75–78 (2019).
10. Blair, J. D., Hockemeyer, D. & Bateup, H. S. Genetically engineered human cortical spheroid models of tuberous sclerosis. *Nat. Med.* **24**, 1568–1578 (2018).
11. Lopez-Tobon, A. et al. Human cortical organoids expose a differential function of GSK3 on cortical neurogenesis. *Stem Cell Rep.* **13**, 847–861 (2019).
12. Pasca, A. M. et al. Human 3D cellular model of hypoxic brain injury of prematurity. *Nat. Med.* **25**, 784–791 (2019).
13. Khan, T. A. et al. Neuronal defects in a human cellular model of 22q11.2 deletion syndrome. *Nat. Med.* **26**, 1888–1898 (2020).
14. Bowles, K. R. et al. ELAVL4, splicing, and glutamatergic dysfunction precede neuron loss in MAPT mutation cerebral organoids. *Cell* **184**, 4547–4563.e17 (2021).
15. Garcia-Ochoa, F., Santos, V. E., Casas, J. A. & Gomez, E. Xanthan gum: production, recovery, and properties. *Biotechnol. Adv.* **18**, 549–579 (2000).
16. Tonnesen, J., Inavalli, V. & Nagerl, U. V. Super-resolution imaging of the extracellular space in living brain tissue. *Cell* **172**, 1108–1121. e15 (2018).
17. Chambers, S. M. et al. Highly efficient neural conversion of human ES and iPS cells by dual inhibition of SMAD signaling. *Nat. Biotechnol.* **27**, 275–280 (2009).
18. Sloan, S. A. et al. Human astrocyte maturation captured in 3D cerebral cortical spheroids derived from pluripotent stem cells. *Neuron* **95**, 779–790.e6 (2017).
19. Yang, X. et al. Kirigami electronics for long-term electrophysiological recording of human neural organoids and assembloids. *Nat. Biotechnol.* **42**, 1836–1843 (2024).
20. Vertesy, A. et al. Gruffi: an algorithm for computational removal of stressed cells from brain organoid transcriptomic datasets. *EMBO J.* **41**, e111118 (2022).
21. He, Z. et al. An integrated transcriptomic cell atlas of human neural organoids. *Nature* **635**, 690–698 (2024).
22. Zhang, Y. et al. Fast and sensitive GCaMP calcium indicators for imaging neural populations. *Nature* **615**, 884–891 (2023).
23. Adam, M. P., Polifka, J. E. & Friedman, J. M. Evolving knowledge of the teratogenicity of medications in human pregnancy. *Am. J. Med. Genet. C* **157C**, 175–182 (2011).
24. Xing, J. et al. In vitro micropatterned human pluripotent stem cell test (microP-hPST) for morphometric-based teratogen screening. *Sci. Rep.* **7**, 8491 (2017).
25. Hande, K. R. Clinical applications of anticancer drugs targeted to topoisomerase II. *Biochim. Biophys. Acta* **1400**, 173–184 (1998).
26. Meng, X. et al. Assembloid CRISPR screens reveal impact of disease genes in human neurodevelopment. *Nature* **622**, 359–366 (2023).
27. Pasca, S. P. et al. A nomenclature consensus for nervous system organoids and assembloids. *Nature* **609**, 907–910 (2022).
28. Negraes, P. D. et al. Altered network and rescue of human neurons derived from individuals with early-onset genetic epilepsy. *Mol. Psychiatry* **26**, 7047–7068 (2021).

29. Boutin, M. E. et al. A multiparametric calcium signal screening platform using iPSC-derived cortical neural spheroids. *SLAS Discov.* **27**, 209–218 (2022).
30. Miura, Y. et al. Engineering brain assembloids to interrogate human neural circuits. *Nat. Protoc.* **17**, 15–35 (2022).
31. Miura, Y. et al. Generation of human striatal organoids and cortico-striatal assembloids from human pluripotent stem cells. *Nat. Biotechnol.* **38**, 1421–1430 (2020).
32. Pantazis, C. B. et al. A reference human induced pluripotent stem cell line for large-scale collaborative studies. *Cell Stem Cell* **29**, 1685–1702 e1622 (2022).
33. Fleck, J. S. et al. Resolving organoid brain region identities by mapping single-cell genomic data to reference atlases. *Cell Stem Cell* **28**, 1177–1180 (2021).
34. Susaki, E. A. et al. Versatile whole-organ/body staining and imaging based on electrolyte-gel properties of biological tissues. *Nat. Commun.* **11**, 1982 (2020).
35. Miura, Y. & Pașca, S.P. Scalable production of human cortical organoids using a biocompatible polymer. Datasets. *NCBI GEO* https://www.ncbi.nlm.nih.gov/geo/query/acc.cgi?acc=GSE232581 (2025).
36. Miura, Y. et al. Scalable production of human cortical organoids using a biocompatible polymer. *Zenodo* https://doi.org/10.5281/zenodo.15092416 (2025).

Acknowledgements

We thank members of the Pașca laboratory at Stanford University for scientific inputs, and N. Eckman for help with viscosity measurement. This work was supported by the Stanford Brain Organogenesis Big Idea Grant from the Wu Tsai Neurosciences Institute (to S.P.P. and S.C.H.), US National Institutes of Health (NIH) BRAINS Award MH107800 (to S.P.P.), R01 EB027171 and R01 MH137333 (to S.C.H.), the NYSCF Robertson Stem Cell Investigator Award (to S.P.P.), the Kwan Research Fund (to S.P.P.), the Coates Foundation (to S.P.P.), the Senkut Research Funds (to S.P.P.), The Ludwig Foundation (to S.P.P.), the Chan Zuckerberg Initiative Ben Barres Investigator Award (to S.P.P.), Stanford Medicine Dean's Fellowship (to Y.M.), the US National Science Foundation (NSF) awards CBET 2033302, DMR 2103812 and DMR 2427971 (to S.C.H.), a TAA Young Investigator Award (to Y.M.), a Stanford Maternal and Child Health Research Institute (MCHRI) Postdoctoral Fellowship (to Y.M.), the Stanford Bio-X Undergraduate Summer Research Program (to S.D.P.), and SNSF Postdoc.Mobility Grant 222016 (to M.A.).

Author contributions

G.N., Y.M. and S.P.P. conceived the project and designed experiments. G.N. performed the screening experiments for biocompatible polymers and drugs. Y.M. carried out differentiation experiments, 3D clearing and staining, immunocytochemistry, single-cell transcriptomics experiments and data analyses. S.D.P. conducted the differentiation experiments, 3D clearing, imaging and image analysis. M.V.T. performed the differentiation experiments, RNA extractions and qPCRs, LDH assay and characterization of organoids. J.G.R., S.S. and S.C.H. selected and prepared biocompatible polymers, and characterized properties of XG-supplemented media. M.A. performed differentiation experiments, immunocytochemistry, 3D clearing, characterization of XG-hCO cultures, and prepared scRNA-seq libraries. J.K. and Z.H. analysed the calcium imaging data. Y.M. and S.P.P. wrote the paper with input from all authors.

Competing interests

G.N. was an employee of Daiichi-Sankyo Co., Ltd, during the duration of this study, but the company did not have any input on the design of experiments and interpretation of the data. Stanford University holds a patent that covers the generation of cortical organoids (US patent 62/477,858), which has been commercially licensed to STEMCELL Technologies. S.P.P. is listed as an inventor on this patent. The other authors declare no competing interests.

Additional information

Extended data is available for this paper at https://doi.org/10.1038/s41551-025-01427-3.

Supplementary information The online version contains supplementary material available at https://doi.org/10.1038/s41551-025-01427-3.

Correspondence and requests for materials should be addressed to Sergiu P. Pașca.

Peer review information *Nature Biomedical Engineering* thanks Woong Sun and the other, anonymous, reviewer(s) for their contribution to the peer review of this work.

https://doi.org/10.1038/s41551-025-01427-3

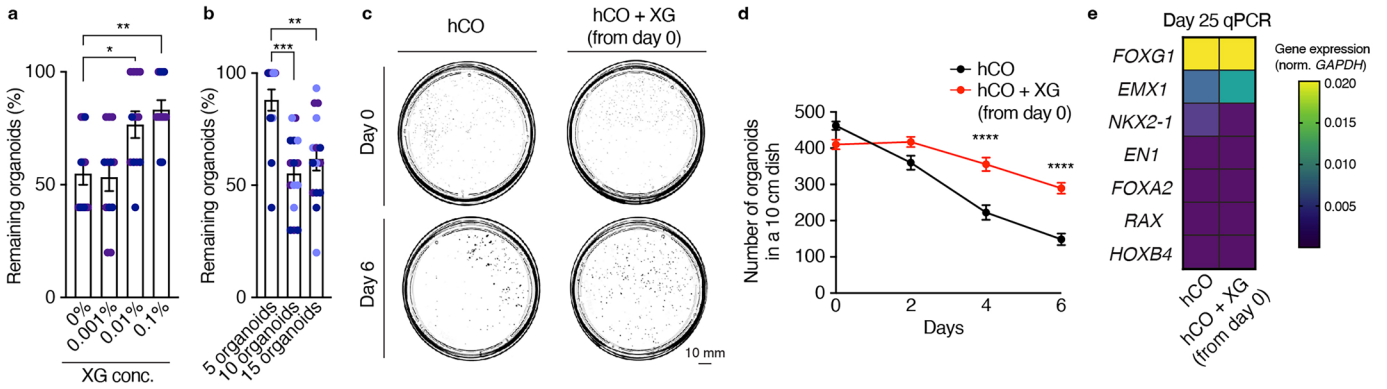

Extended Data Fig. 1 | Scalable organoid culture using biocompatible polymers. (**a**) Quantification of remaining organoids at day 25 of culture following supplementation with 0%, 0.001%, 0.01%, and 0.1% XG; $n = 12$ wells for each condition. One-way ANOVA result: $^{***}P = 0.0003$, $F = 0.8485_{(5,66)}$, $P = 0.99$ Dunn's multiple comparisons test for 0% versus 0.001%, $^{*}P = 0.03$ for 0% versus 0.01%, $^{**}P = 0.003$ for 0% versus 0.1%. Data show mean ± s.e.m. (**b**) Quantification of remaining organoids at day 25 following supplementation with 0.1% XG; $n = 15$ wells conditions starting with 5 organoids, 10 organoids or 15 organoids (3 hiPS cell lines). Kruskal–Wallis test, ANOVA result; $^{***}P = 0.0002$, $^{***}P = 0.0003$ with Dunn's multiple comparisons test for 5 organoids versus 10 organoids, $^{**}P = 0.0046$ for 5 organoids vs. 15 organoids, $P > 0.9999$ for 10 organoids vs. 15 organoids. Data show mean ± s.e.m. (**c**) Representative images of 10 cm dishes including hCO and hCO +XG at day 0 (top) and day 6 (bottom). (**d**) Number of organoids at days 0, 2, 4 and 6. $n = 24$ plates for control and $n = 24$ (days 0 and 4), 23 (day 2), and 22 (day 4) for hCO + XG. Two-tailed unpaired t-test, $^{****}P < 0.0001$. Data show mean ± s.e.m. (**e**) qPCR of hCO and hCO + XG (from day 0) at day 25; $n = 16$–22 organoids for untreated hCO, $n = 10$–11 organoids for hCO + XG from 3 differentiation experiments including 4 hiPS cell lines. Two-tailed Mann-Whitney test, $P = 0.07$ for *FOXG1*, $P = 0.34$ for *EN1*, $P = 0.09$ for *EMX1*, $P = 0.07$ for *NKX2.1*, $P = 0.72$ for *FOXA2*, $P = 0.93$ for *RAX*, $P = 0.30$ for *HOXB4*. Data show mean.

https://doi.org/10.1038/s41551-025-01427-3

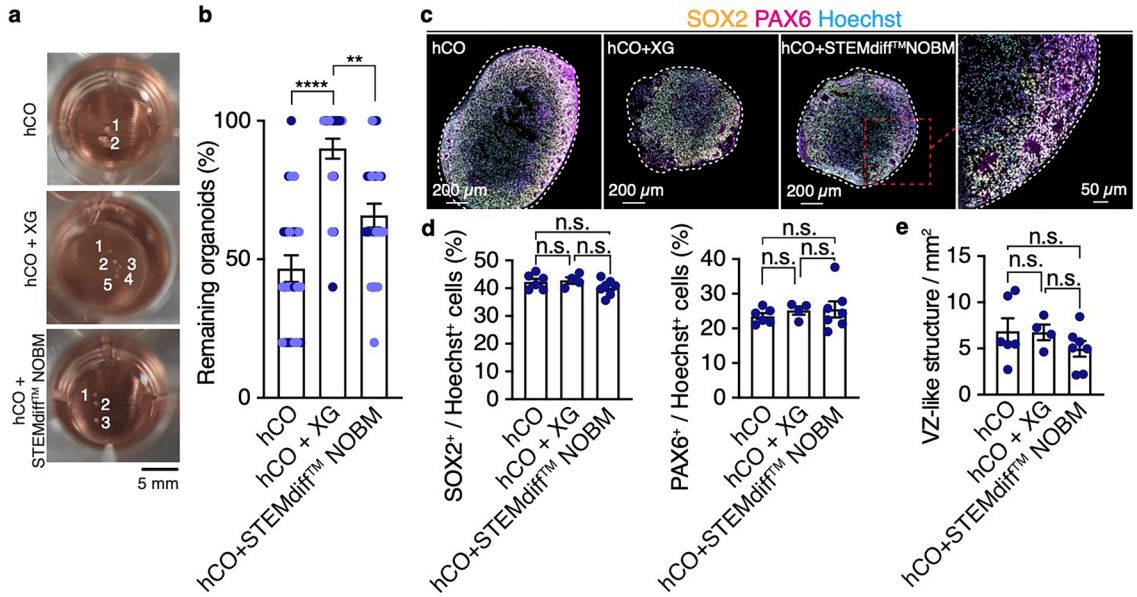

Extended Data Fig. 2 | Reduced fusion of organoids following XG treatment. (**a**) Representative images of untreated hCO (top), xanthan gum-supplemented (hCO + XG, middle) and STEMdiff™ Neural Organoid Basal Medium 2 cultured hCO (hCO + STEMdiff™ NOBM, bottom). Scale bar: 5 mm. (**b**) Graph showing remaining organoids after 5 days of culture; $n = 24$ wells tested for untreated hCO, $n = 24$ wells tested for hCO + XG, $n = 24$ wells tested for hCO + ST from 2 differentiation experiments of 2 hiPS cell lines. Kruskal–Wallis test, ANOVA result: $^{****}P < 0.0001$, $^{****}P < 0.0001$ with multiple comparisons for untreated hCO versus hCO + XG, $^{**}P = 0.002$ for hCO + XG versus hCO + ST. Data show mean ± s.e.m. (**c**) Immunostaining for SOX2 (yellow), PAX6 (magenta), and Hoechst (cyan) in hCO, hCO+XG, and hCO + ST at day 25. Scale bar: 200 µm, and 50 µm for an inset. (**d**) Quantified data of SOX2$^+$ / Hoechst$^+$ cells and PAX6$^+$ / Hoechst$^+$ cells in untreated hCO, hCO + XG and hCO + ST at day 25. $n = 6$ organoids for untreated hCO, $n = 4$ organoids for hCO + XG and $n = 7$ organoids for hCO + ST from 2 differentiation experiments of 1 hiPS cell line. Ordinary one-way ANOVA, $P = 0.25$ for SOX2$^+$ / Hoechst$^+$ cells and $P = 0.70$ for PAX6$^+$ / Hoechst$^+$ cells. Data show mean ± s.e.m. (**e**) Density of progenitor ventricular-like zones. $n = 6$ for hCO, $n = 4$ for hCO + XG, and $n = 7$ for hCO + ST. Ordinary one-way ANOVA, $P = 0.37$. Data show mean ± s.e.m.

https://doi.org/10.1038/s41551-025-01427-3

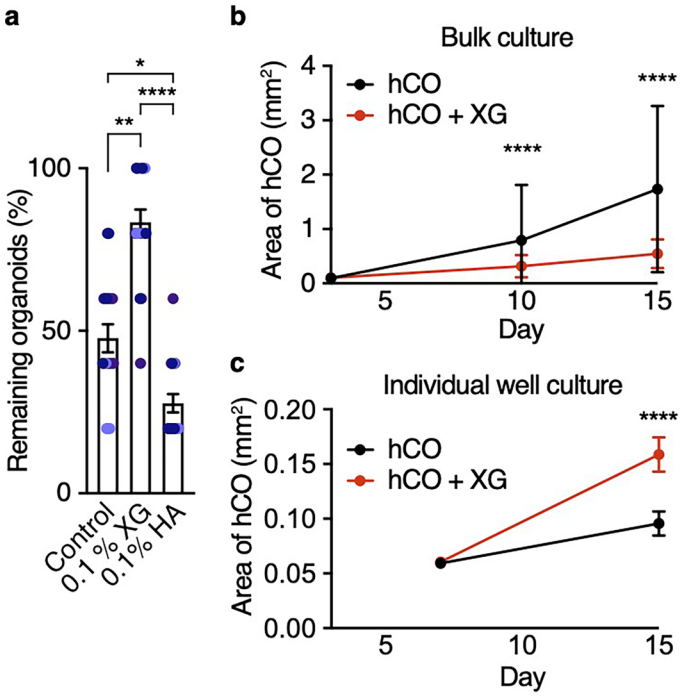

Extended Data Fig. 3 | Characterization of XG-hCO. (**a**) Quantification of remaining organoids at day 25 of culture following supplementation with 0.1% XG or 0.1% HA; $n = 18$ wells for each condition (3 hiPS cell lines). Kruskal–Wallis test, ANOVA result: $^{****}P < 0.0001$, $^{**}P = 0.0013$ with Dunn's multiple comparisons test for control versus 0.1% XG, $^{*}P = 0.047$ for control versus 0.1% HA, $^{****}P < 0.0001$ for 0.1% XG versus 0.1% HA. Data show mean ± s.e.m. (**b**) Area of hCO at day 3, 10 and 15 cultured with XG or regular culture medium; $n = 409$ organoids for untreated hCO at day 3, $n = 516$ organoids for hCO +XG at day 3, $n = 208$ organoids for untreated hCO at day 10, $n = 479$ organoids for hCO + XG at day 10, $n = 143$ organoids for untreated hCO at day 15, $n = 308$ organoids for hCO + XG at day 15, from 4 differentiation experiments including 4 hiPS cell lines. Two-way ANOVA $^{****}P < 0.0001$, $P = 0.99$ for day 3, $^{****}P < 0.0001$ for day 10, $^{****}P < 0.0001$ for day 15 with Šidák multiple comparison tests. Data show mean ± s.d. (**c**) Area of hCO at day 7, and 15 cultured with XG or regular culture medium in individual well culture experiments; $n = 81$ organoids for untreated hCO at day 7, $n = 80$ organoids for hCO +XG at day 7, $n = 74$ organoids for untreated hCO at day 15, $n = 64$ organoids for hCO +XG at day 15 from 3 differentiation experiments including 3 hiPS cell lines. Two-way ANOVA $^{***}P = 0.0004$, $P = 0.99$ for day 7, and $^{****}P < 0.0001$ for day 15 with Šidák multiple comparison test. Data show mean ± s.d.

https://doi.org/10.1038/s41551-025-01427-3

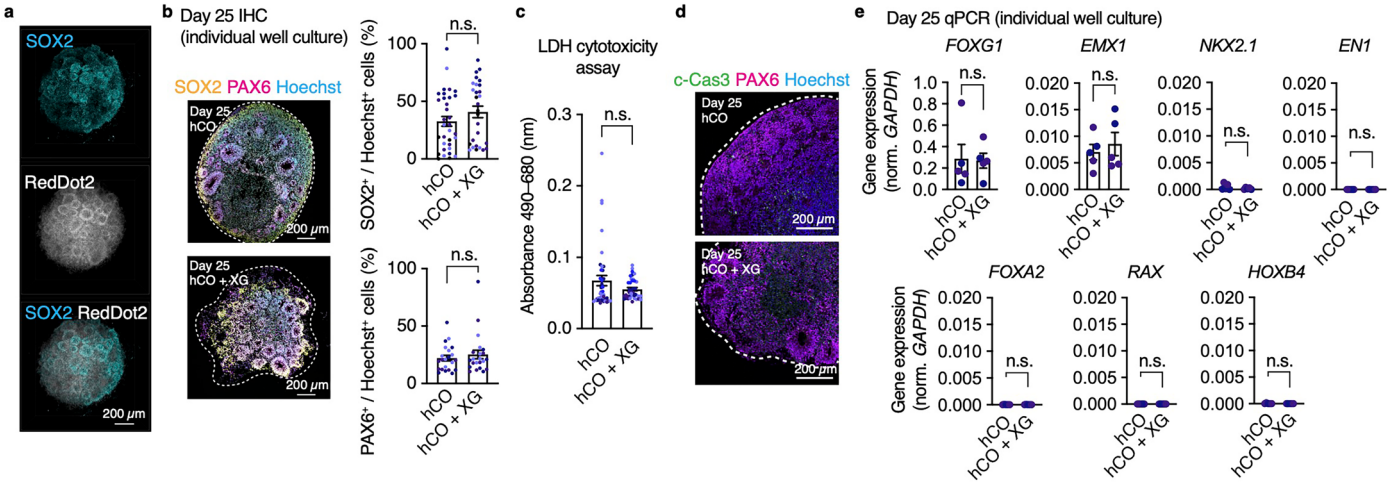

Extended Data Fig. 4 | Cortical patterning and cytotoxicity analysis of XG-hCO. (**a**) 3D immunostaining of CUBIC-cleared XG-hCO. SOX2: Cyan, RedDot2: gray. Scale bar: 200 µm. (**b**) Immunostaining for SOX2 (yellow), PAX6 (magenta), and Hoechst (cyan), and quantification of SOX2$^+$ / Hoechst$^+$ cells and PAX6$^+$ / Hoechst$^+$ cells in untreated hCO and hCO + XG at day 25. n = 33 organoids for untreated hCO, n = 28 organoids for hCO + XG from 3 differentiation experiments of 3 hiPS cell lines for SOX2, and n = 22 organoids for untreated hCO, n = 22 organoids for hCO + XG from 2 differentiation experiments of 3 hiPS cell lines for PAX6. Two-tailed Mann-Whitney test, P = 0.17 for SOX2 and P = 0.71 for PAX6. Scale bar: 200 µm. Data show mean ± s.e.m. (**c**) LDH cytotoxicity assay for day 25 hCO or hCO + XG; n = 39 wells for untreated hCO, n = 39 wells for hCO + XG from 3 differentiation experiments including 4 hiPS cell lines. Two-tailed Mann-Whitney test, P = 0.64. Data show mean ± s.e.m. (**d**) Immunostaining of cleaved Caspase-3 (c-Cas3) on day 25 untreated hCO and hCO + XG. Scale bar: 200 µm. (**e**) qPCR of hCO and XG-hCO cultured as single organoids; n = 5 organoids for hCO, n = 5 organoids for hCO + XG from 4 differentiation experiments of 2 hiPS cell lines. Two-tailed Mann-Whitney test, P = 0.54 for *FOXG1*, P > 0.9999 for *EN1*, P = 0.84 for *EMX1*, P = 0.69 for *NKX2.1*, P = 0.69 for *FOXA2*, P = 0.16 for *RAX*, P = 0.55 for *HOXB4*. Data show mean ± s.e.m.

https://doi.org/10.1038/s41551-025-01427-3

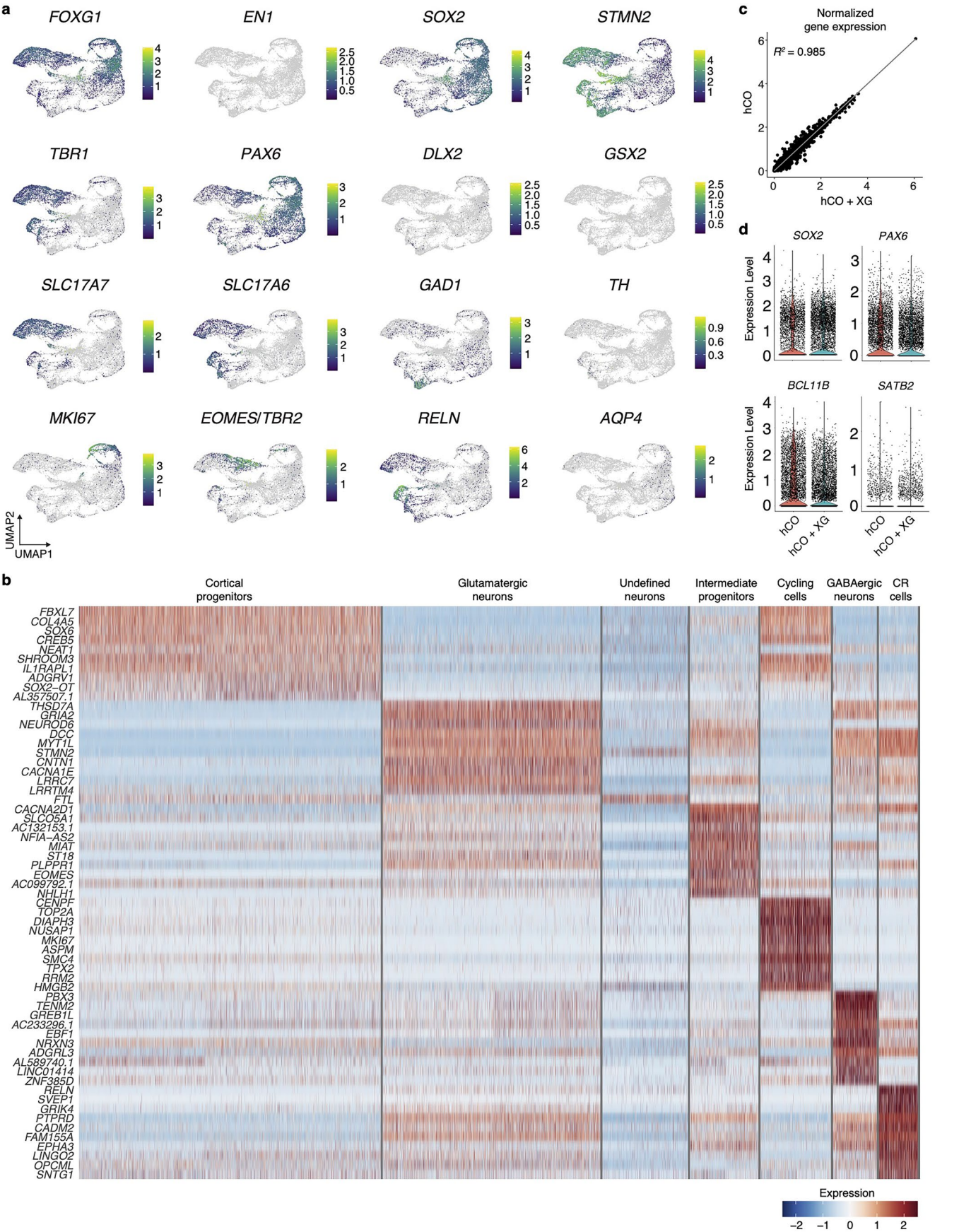

Extended Data Fig. 5 | Single-cell RNAseq analysis of XG-hCO. (**a**) UMAP projection of cell type makers of hCO, and XG-supplemented hCO. (**b**) Heatmap showing differentially expressed genes per each cluster. (**c**) Plot showing the Pearson's correlation of the normalized average gene expression between untreated hCO and hCO + XG. (**d**) Violin plots showing gene expressions of *SOX2*, *PAX6*, *BCL11B*, and *SATB2* in hCO and hCO + XG.

https://doi.org/10.1038/s41551-025-01427-3

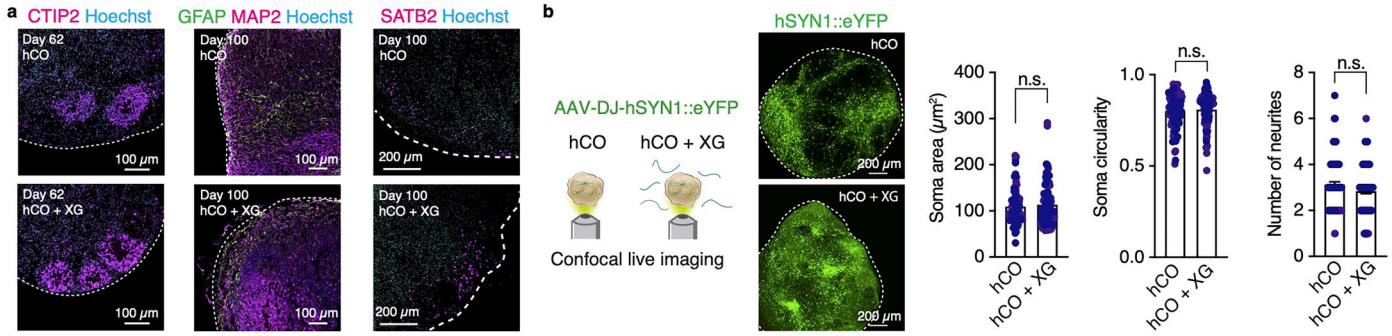

Extended Data Fig. 6 | Cortical layer marker expression and neuronal morphology in XG-hCO. (**a**) Immunostaining for CTIP2 (magenta) and Hoechst (cyan) at day 62 (left panels, $n = 3$ for hCO and $n = 4$ for XG-hXO), GFAP (green), MAP2 (magenta) and Hoechst (cyan) at day 100 (middle panels, $n = 8$ for hCO and $n = 6$ for XG-hXO), SATB2 (magenta) and Hoechst (cyan) at day 100 (right panels, $n = 6$ for hCO and $n = 6$ for XG-hXO) in hCO and XG-hCO. Scale bars: 100 µm for left and middle panels, and 200 µm for right panels. (**b**) Confocal live Imaging of virally labeled eYFP$^+$ neurons in hCO and XG-hCO. Representative images of neurons expressing eYFP in hCO and hCO + XG. Quantification of soma area, soma circularity and the number of neurites. $n = 95$ neurons from 5 organoids for hCO, $n = 100$ neurons from 6 organoids for hCO + XG from 2 differentiation experiments of 2 hiPS cell lines. Two-tailed Mann-Whitney test, $P = 0.86$ for soma area, $P = 0.52$ for soma circularity, and $P = 0.15$ for the number of neurites. Data show mean ± s.e.m.

https://doi.org/10.1038/s41551-025-01427-3

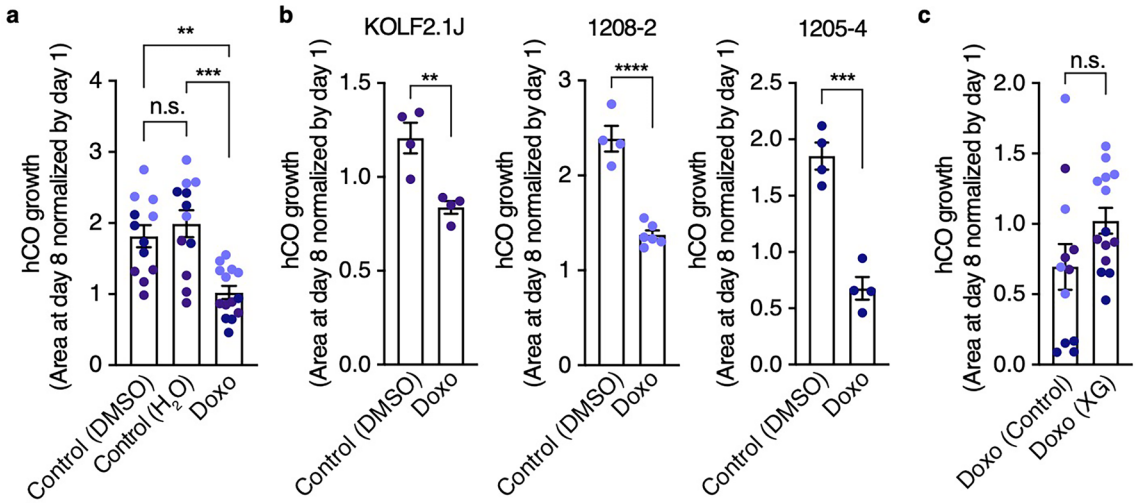

Extended Data Fig. 7 | Effects of doxorubicin on hCO. (**a**) Organoid growth ratio of hCO treated with Doxo for 8 days or DMSO or H_2O treated hCO; $n = 12$ organoids for control (DMSO), $n = 12$ organoids for control (H_2O), $n = 14$ organoids for Doxo treated hCO from 3 hiPS cell lines. One-way ANOVA: $F = 2.310_{(2,35)}$, $P = 0.69$ with Tukey's multiple comparisons test for control (DMSO) versus control (H_2O), $^{**}P = 0.0013$ for control (DMSO) versus Doxo, $^{***}P = 0.0001$ for control (H_2O) versus Doxo. Data show mean ± s.e.m. (**b**) Organoid growth ratio of hCO treated with Doxo per hiPS cell lines from data in (**e**); $n = 4$ organoids for each condition (KOLF2.1J and 1205-4), $n = 4$ organoids for control and $n = 6$ organoids for Doxo-treated hCO (1208-2); two-tailed unpaired t-test, $^{**}P = 0.0058$ for KOLF2.1J, $^{****}P < 0.0001$ for 1208-2, and $^{***}P = 0.0003$ for 1205-4. Data show mean ± s.e.m. (**c**) Organoid growth ratio of hCO treated with Doxo added to control medium or XG-supplemented medium; $n = 12$ organoids for Doxo (Control), $n = 14$ organoids for Doxo (XG) including 3 hiPS cell lines. Two-tailed unpaired t-test, $P = 0.08$. Data show mean ± s.e.m.

nature portfolio

Corresponding author(s): Sergiu P. Pașca

Last updated by author(s): Mar 30, 2025

Reporting Summary

Nature Portfolio wishes to improve the reproducibility of the work that we publish. This form provides structure for consistency and transparency in reporting. For further information on Nature Portfolio policies, see our Editorial Policies and the Editorial Policy Checklist.

Statistics

For all statistical analyses, confirm that the following items are present in the figure legend, table legend, main text, or Methods section.

n/a	Confirmed	
☐	☒	The exact sample size (*n*) for each experimental group/condition, given as a discrete number and unit of measurement
☐	☒	A statement on whether measurements were taken from distinct samples or whether the same sample was measured repeatedly
☐	☒	The statistical test(s) used AND whether they are one- or two-sided *Only common tests should be described solely by name; describe more complex techniques in the Methods section.*
☒	☐	A description of all covariates tested
☐	☒	A description of any assumptions or corrections, such as tests of normality and adjustment for multiple comparisons
☐	☒	A full description of the statistical parameters including central tendency (e.g. means) or other basic estimates (e.g. regression coefficient) AND variation (e.g. standard deviation) or associated estimates of uncertainty (e.g. confidence intervals)
☐	☒	For null hypothesis testing, the test statistic (e.g. *F*, *t*, *r*) with confidence intervals, effect sizes, degrees of freedom and *P* value noted *Give P values as exact values whenever suitable.*
☒	☐	For Bayesian analysis, information on the choice of priors and Markov chain Monte Carlo settings
☒	☐	For hierarchical and complex designs, identification of the appropriate level for tests and full reporting of outcomes
☐	☒	Estimates of effect sizes (e.g. Cohen's *d*, Pearson's *r*), indicating how they were calculated

Our web collection on statistics for biologists contains articles on many of the points above.

Software and code

Policy information about availability of computer code

Data collection	The BZ-X Analyzer (KEYENCE) and LAS-X (Leica, Version 4.5.0.25531) softwares were used for acquiring the microscopy data. m-VROC software (v3.1.5) was used to collect viscosity data.
Data analysis	The GraphPad Prism (Version 9.3.1) was used for statistical analyses. ImageJ (Version 2.3.0/1.53f), Imaris (Version 9.6), Matlab (Version 9.13.0.2105380, R2022b) python (Version3.9) and Spyder (Version 5) were used for image quantification and processing. R (Version 4.1.1) was used for plotting histogram and single cell RNA-seq analysis. Seurat (Version 4.1.2) and VoxHunt (Version 1.0.0) were used for single cell RNA-seq analysis.

For manuscripts utilizing custom algorithms or software that are central to the research but not yet described in published literature, software must be made available to editors and reviewers. We strongly encourage code deposition in a community repository (e.g. GitHub). See the Nature Portfolio guidelines for submitting code & software for further information.

Data

Policy information about availability of data

All manuscripts must include a data availability statement. This statement should provide the following information, where applicable:

- Accession codes, unique identifiers, or web links for publicly available datasets
- A description of any restrictions on data availability
- For clinical datasets or third party data, please ensure that the statement adheres to our policy

Gene expression data is available in the Gene Expression Omnibus (GEO) under accession numbers GSE232581. The data in this study are provided in the Source Data files and available on request from the corresponding author.

Research involving human participants, their data, or biological material

Policy information about studies with human participants or human data. See also policy information about sex, gender (identity/presentation), and sexual orientation and race, ethnicity and racism.

Reporting on sex and gender	N/A
Reporting on race, ethnicity, or other socially relevant groupings	N/A
Population characteristics	N/A
Recruitment	N/A
Ethics oversight	N/A

Note that full information on the approval of the study protocol must also be provided in the manuscript.

Field-specific reporting

Please select the one below that is the best fit for your research. If you are not sure, read the appropriate sections before making your selection.

☒ Life sciences ☐ Behavioural & social sciences ☐ Ecological, evolutionary & environmental sciences

For a reference copy of the document with all sections, see nature.com/documents/nr-reporting-summary-flat.pdf

Life sciences study design

All studies must disclose on these points even when the disclosure is negative.

Sample size	Sample sizes were estimated empirically, based on previous studies (Yoon et al., Nature Methods 2019; Khan et al., Nature Medicine 2020; Birey et al, Cell Stem Cell 2022; Miura et al, Nature Biotechnology 2020; Meng et al, Nature 2023; Chen et al, Nature 2024)
Data exclusions	For testing effects of drugs, hCOs that fused in wells were excluded from the analysis.
Replication	Most experiments were performed using 2-5 hiPS cell lines. For each assay, multiple hCOs from 1-4 differentiation experiments were used.
Randomization	hCOs were randomly picked for each assay. 2-5 hiPS cell lines were used for most experiments.
Blinding	Investigators were blinded for FDA-drug screening experiments and image quantification. Blinding was not used or was not relevant for other experiments.

Reporting for specific materials, systems and methods

We require information from authors about some types of materials, experimental systems and methods used in many studies. Here, indicate whether each material, system or method listed is relevant to your study. If you are not sure if a list item applies to your research, read the appropriate section before selecting a response.

Materials & experimental systems

n/a	Involved in the study
☐	☒ Antibodies
☐	☒ Eukaryotic cell lines
☒	☐ Palaeontology and archaeology
☒	☐ Animals and other organisms
☒	☐ Clinical data
☒	☐ Dual use research of concern
☒	☐ Plants

Methods

n/a	Involved in the study
☒	☐ ChIP-seq
☒	☐ Flow cytometry
☒	☐ MRI-based neuroimaging

Antibodies

Antibodies used

anti-SOX2 (rabbit, Cell Signaling Technology, 3579, 1:300 dilution, Lot#8)
anti-PAX6 (mouse, DSHB, PAX6 1:200 dilution)
anti-Cleaved Caspase-3 (Asp175) (rabbit, Cell Signaling Technology, 9661, 1:200 dilution, Lot#45)
FITC Anti-CTIP2 antibody [25B6] (rat, abcam, ab123449, 1:100 dilution)
anti-GFAP (rabbit, DAKO, Z0334, 1:1000 dilution)
anti-MAP2 (guinea pig, Synaptic Systems 188 004, 1:200 dilution)
anti-SATB2 (mouse, Abcam: AB51502, 1:50 dilution)
Alexa Fluor dyes, donkey anti-rabbit IgG (H&L) highly cross-adsorbed secondary antibody, Alexa Fluor 488 (Thermo Fisher Scientific, A-21206, 1:500–1:1000 dilution)
Alexa Fluor dyes, donkey anti-mouse IgG (H&L) highly cross-adsorbed secondary antibody , Alexa Fluor 568 (Thermo Fisher Scientific, A10037, 2110843, 1:500–1:1000 dilution)
Alexa Fluor® 647 AffiniPure Donkey Anti-Guinea Pig IgG (H+L) (Jackson ImmunoResearch, 706-605-148, 1:500–1:1000 dilution)

Validation

We have used and/or validated some of the antibodies in our previous studies (Pasca et al., Nature Methods 2015; Yoon et al., Nature Methods 2018, Miura et al., Nature Biotechnology 2020: anti-SOX2, PAX6, anti-Cleaved Caspase-3, anti-CTIP2, anti-GFAP, anti-MAP2, anti-SATB2.

Eukaryotic cell lines

Policy information about cell lines and Sex and Gender in Research

Cell line source(s)

hiPS cell lines were derived at Stanford University with IRB approval and written consent, except for the KOLF2.1J hiPS cell line which was obtained from the Jackson Laboratory.

Authentication

hiPS cell lines were authenticated by SNP arrays.

Mycoplasma contamination

All hiPS cell lines were regularly tested and maintained Mycoplasma free.

Commonly misidentified lines
(See ICLAC register)

No commonly misidentified cell lines were used.

Plants

Seed stocks

N/A

Novel plant genotypes

N/A

Authentication

N/A